



Crystal network formation in organic solar cells

J.J. Dittmer^{a,*}, R. Lazzaroni^b, Ph. Leclère^b, P. Moretti^b,
M. Granström^a, K. Petritsch^a, E.A. Marseglia^a, R.H. Friend^a,
J.L. Brédas^b, H. Rost^c, A.B. Holmes^c

^a*Optoelectronics Group, Cavendish Laboratory, University of Cambridge, Madingley Road,
Cambridge, CB3 0HE, UK*

^b*Service de Chimie des Matériaux Nouveaux, Université de Mons-Hainaut, B-7000 Mons, Belgium*

^c*Melville Laboratory for Polymer Synthesis, Pembroke Street, Cambridge, CB2 3RA, UK*

Accepted 25 May 1999

Abstract

We have studied the effects of annealing on performance and morphology of photovoltaic devices using blends of two organic semiconductors: a conjugated polymer and a soluble perylene derivative. The efficiency of such photovoltaic cells has been determined. The effect of temperature on blend morphology has been investigated for actual device films. Annealing leads to the formation of micron size perylene crystals and an enhancement of the quantum efficiency. This enhancement has been attributed to the formation of an electron conducting perylene crystal network. © 2000 Elsevier Science B.V. All rights reserved.

Keywords: MEH-PPV; Conjugated polymers; Perylene; Donor–acceptor blends; Organic solar cells; AFM tapping mode; Phase detection

1. Introduction

State-of-the-art monocrystalline silicon solar cells can harvest up to about 24% of the incoming solar energy (power efficiency) [1]. However, manufacturing these cells requires many energy intensive processing steps at high temperatures (400–1400°C), leading to relatively high production costs and low-energy harvesting factors (energy

* Corresponding author. Tel.: +44-1223-337286; fax: +44-1223-353397.

E-mail address: jjd24@cam.ac.uk (J.J. Dittmer)

generated during lifetime divided by energy invested for production). Considerably less production energy is necessary if organic semiconductors are used because of simpler fabrication methods. Organic conjugated polymers combine the optoelectronic properties of semiconductors with the excellent mechanical and processing properties of polymeric materials. They can be deposited from solution at low temperature ($< 200^{\circ}\text{C}$) onto e.g. flexible substrates using simple and cheap deposition methods such as spin or blade coating. Since the discovery of electroluminescence in conjugated polymers [2], this class of materials has been used to build light-emitting diodes [2–6], field effect transistors [7–11], optically pumped lasers [12,13] and photovoltaic diodes [14–17].

In these materials, incident photons are believed to create bound electron–hole pairs [18]. These so-called excitons have to dissociate into free charges in order to be transported to the electrodes. However, the exciton diffusion range in a typical conjugated polymer is only about 10 nm [19]. Exciton dissociation, i.e. charge transfer occurs efficiently at interfaces between certain metals and organic semiconductors [20,21] and at interfaces between organic semiconductors with different electron affinities and ionisation potentials [19,22]. The electron will then be accepted by the material with the higher electron affinity (electron acceptor) and the hole by the material with the lower ionisation potential (hole acceptor) [14,23]. In order to be useful for photovoltaic applications, the excitons have to reach such an interface before it decays radiatively or non-radiatively. One way of creating a large interfacial area on a scale similar to the exciton diffusion range is to mix an electron donor with an electron acceptor material. Solar cells based on conjugated polymer blends which form an interpenetrating network have shown quantum efficiencies of up to 30% corresponding to a calculated AM1.5 efficiency of 2% [24]. Whereas charge separation seems to be efficient in these polymer networks, charge transport still remains a limiting factor to device efficiency due to imperfect network structures and low charge carrier mobilities especially for negative charges.

The aim of our work has been to investigate the impact of morphology on photovoltaic performance. Since blend morphology has been shown to have an

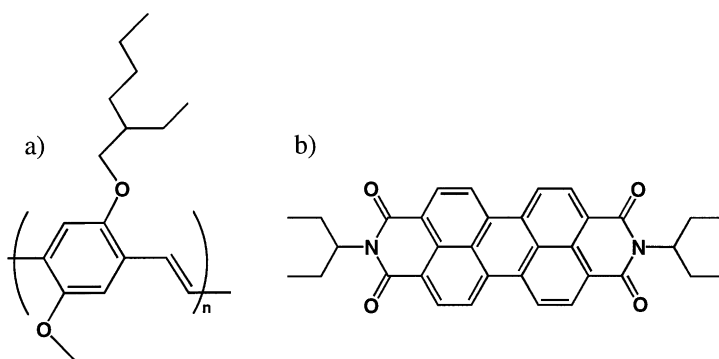


Fig. 1. Chemical structure of (a) poly(2-methoxy-5-(2'-ethyl-hexyloxy)-p-phenylene vinylene), MEH-PPV, and (b) N,N'-bis(1-ethylpropyl)-3,4:9,10-perylene bis(tetracarboxyl diimide) referred to as perylene.

important effect on the efficiency of polymer solar cells, a better understanding of how to predict or even control this blend morphology is essential. For the work presented below the conjugated polymer MEH-PPV (Fig. 1a), which is soluble in common organic solvents, was used as the electron donor and hole transport material and a soluble perylene derivative purchased from Synthec (Germany) was chosen as the electron acceptor and electron transport medium (Fig. 1b).

2. Experimental

Films of pristine MEH-PPV and perylene as well as different weight ratios of perylene/MEH-PPV blends were fabricated by spin-coating from solution onto glass substrates which were previously coated with a transparent electrode consisting of indium tin oxide (ITO), or onto quartz substrates for photoluminescence (PL) efficiency measurements. The aluminium (Al) top electrode, which typically had a thickness of about 100 nm, was deposited by thermal evaporation in vacuo at pressures of about 3×10^{-6} mbar onto the organic layer. All other fabrication steps were carried out under nitrogen atmosphere to minimise effects of water and oxygen on MEH-PPV. The films were protected from blue and ultraviolet light except during measurements. The absolute PL efficiency was determined using an integrating sphere [25] coupled via a liquid light-guide to an Oriel InstaSpec IV spectrophotometer. The samples were excited by an argon ion laser at a wavelength of 488 nm. The method developed by de Mello et al. was adapted for measuring small PL efficiencies [26].

Measurements of the spectral response were carried out on devices fabricated according to the scheme depicted in Fig. 2. The devices were illuminated from the ITO side at intensities of the order of 0.1 mW/cm^2 using a tungsten lamp, dispersed by a Bentham M300 single-grating monochromator. Quantum efficiencies were determined by normalisation with a calibrated silicon photodiode. Electrical data were taken and bias was applied using a Keithley 237 source-measure unit. Current–voltage characteristics were measured in the dark and using narrow lines from the monochromator. Absorption spectra were measured with a Hewlett-Packard 8453 UV-Vis spectrometer. Film thickness was determined using a Dektak IIa profilometer. The morphology of the organic films was investigated by means of a Nanoscope III atomic force microscope (AFM) used in the tapping mode (TM) with phase detection imaging. The AFM study was carried out on the actual devices for

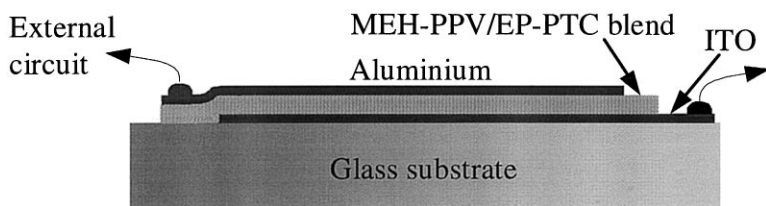


Fig. 2. Device architecture of photovoltaic cell.

which the spectral response had been measured beforehand. Thermal treatment was performed on a high precision hot stage, which was operated inside a nitrogen filled glovebox to minimise effects of oxygen and water which can alter the electronic properties of MEH-PPV [27]. Devices were heated to the desired temperature at a constant rate of $10^{\circ}\text{C}/\text{min.}$ and annealed for 1 h. Cooling was carried out on the same hot stage, but outside the glovebox using liquid nitrogen for cooling. The devices were kept under nitrogen atmosphere during the entire treatment.

3. Results and discussion

3.1. Photoluminescence quenching

Fig. 3 shows the absolute PL efficiency as a function of the weight percentage of perylene in the blend. The PL efficiency is quenched by a factor of more than 300 for a 30 : 70 MEH-PPV : perylene blend with respect to pristine MEH-PPV indicating that there is essentially no radiative exciton decay in these blends.

Thus, every exciton created in the bulk is affected by the presence of the perylene. This implies that the perylene must be dispersed intimately throughout the polymer. After photoexcitation, the exciton may undergo either charge transfer, which is the desired process in photovoltaic cells, or energy transfer as it reaches an interface between the two materials. Energy transfer followed by radiative recombination can be ruled out because the PL efficiency of both materials is quenched in the blend. Therefore charge transfer and energy transfer followed by non-radiative decay are the possibilities that remain. The latter possibility can be ruled out, if significant photocurrent enhancement is observed in the blend device.

3.2. Quantum efficiency

The external quantum efficiency (EQE) spectrum of an ITO/perylene : MEH-PPV (70 : 30) blend/Al photovoltaic cell is shown in Fig. 4. The EQE shows a maximum of

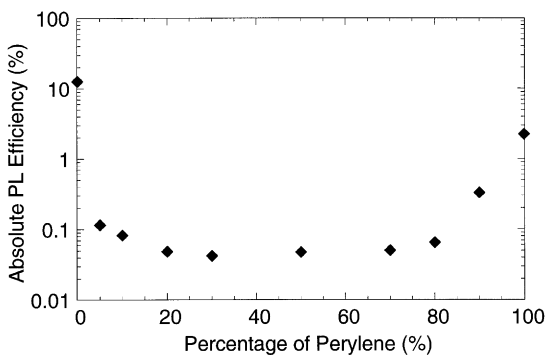


Fig. 3. The absolute PL efficiency for scattered light in blends of MEH-PPV and perylene as a function of perylene weight percentage.

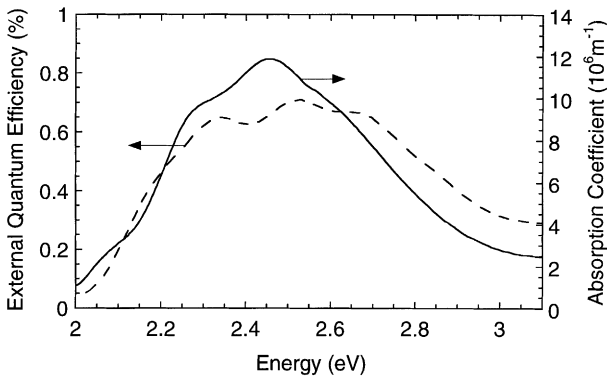


Fig. 4. External quantum efficiency (electrons per incident photon) of an ITO/perylene:MEH-PPV (70:30) blend/Al photovoltaic cell under short circuit conditions (dashed line). The device was illuminated through the ITO electrode. The absorption spectrum of the same device corrected for substrate influences is also shown (solid line). The device thickness was determined to be approximately 100 nm.

0.71% at 2.52 eV flanked by two shoulders at 2.34 and 2.66 eV. The EQE is enhanced by a factor of about 18 with regard to devices using pristine MEH-PPV as the active material, which show an EQE of 0.04% [14].

Together with the efficient PL quenching, this considerable enhancement in photocurrent has to be attributed to charge transfer taking place between MEH-PPV and the perylene. After charge transfer has occurred, the two charges can then travel to the respective electrodes driven by the internal electric field caused by the difference in work function of the two electrodes.

3.3. Current–voltage characteristics

The corresponding current–voltage characteristics are shown in Fig. 5. The open-circuit voltage (V_{oc}) lies at about 370 mV. The rectification ratio at 1 V in the dark is around 10^2 and the fill factor (FF) amounts to 44% under illumination at 540 nm at an intensity of 0.15 mW/cm^2 . This fill factor for the MEH-PPV/perylene blend device is considerably higher than the fill factor for a blend of MEH-PPV and a cyano-substituted PPV derivative at similar light intensity, which lies around 29% [28].

3.4. Morphology

The morphology of pristine and heat treated perylene/MEH-PPV blend devices is shown in Fig. 6. Crystals that are typically of the order of $1 \mu\text{m}$ in size can be distinguished within a continuous film for the pristine device in Fig. 6a. The crystals may be attributed to the perylene, as the small molecule is much more likely to crystallise than the polymer. The shape of these crystals also closely resembles that of pure perylene crystals observed on a slightly larger scale under an optical microscope.

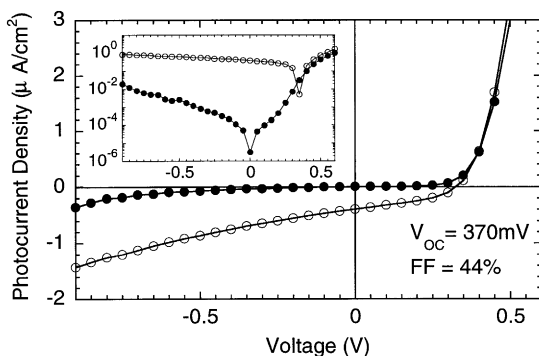


Fig. 5. Current–voltage characteristics of an ITO/perylene : MEH-PPV (70 : 30) blend/Al device measured in the dark (filled circles) and under illumination at 540 nm at an intensity of 0.15 mW/cm² (open circles). The active area of the photovoltaic cell was 2.5 mm². The inset shows the same data as a semi-logarithmic plot.

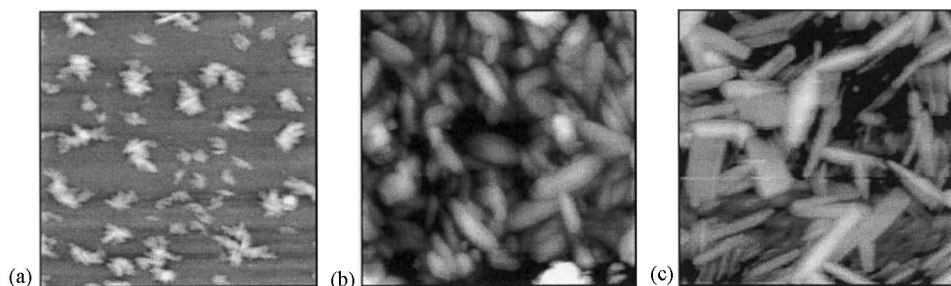


Fig. 6. 5 μm × 5 μm AFM-TM images of 70 : 30 perylene : MEH-PPV blend devices (a) before and (b) after annealing at 110°C and (c) at 200°C.

There is strong evidence, however, that not all the perylene is present in crystalline form: Firstly, Fig. 7 shows an AFM-TM image of the same sample as in Fig. 6a taken in between the crystals on a much smaller scale. The morphology of the film differs from that of a pristine MEH-PPV film. The topography image in Fig. 7 shows the main features of the PDI with inverse contrast. It is important to notice that small domains within a continuous morphology are visible in the PDI, which is an indication of phase separation. The approximate size of the domains is 50 nm, which approaches the desired dimensions for charge separation given by twice the exciton diffusion range (~ 20 nm). Secondly, AFM-TM images of different blend ratios have been recorded. Devices with up to 50% by weight of the perylene showed no crystals. This implies that a large amount of the perylene can be dissolved or dispersed in MEH-PPV.

The effect of heat treatment on the film morphology was investigated for different devices annealed at 75°C, 95°C, 110°C, 150°C, 200°C, and 225°C. With increasing

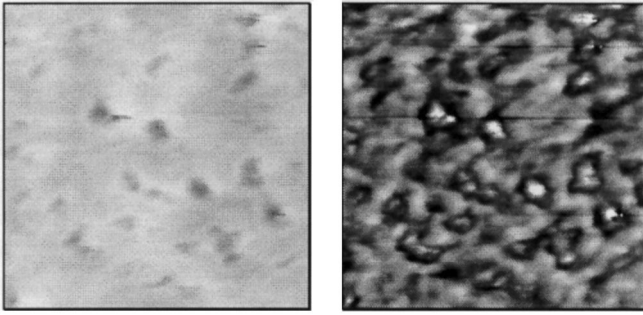


Fig. 7. 300×300 nm AFM-TM images (left: topography; right: phase detection image (PDI)) of the continuous film in the untreated device providing evidence for phase separation. Contrast in the PDI is due to variations in viscoelasticity.

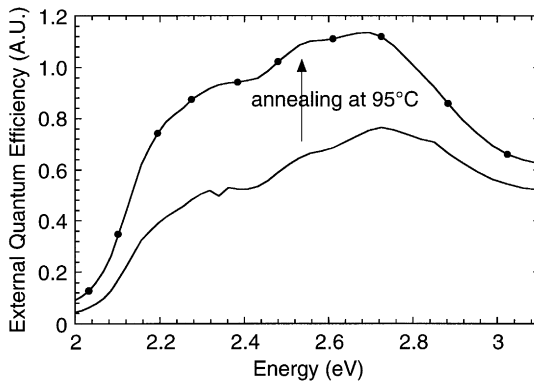


Fig. 8. EQE of an ITO/perylene : MEH-PPV (70 : 30) blend/Al device before (solid line) and after (dotted line) annealing at 95°C . The device thickness was about 165 nm.

temperature, the lamellar crystals increase in number and grow in size from about $1 \mu\text{m}$ to between 4 and $10 \mu\text{m}$. The AFM-TM images for the devices annealed at 110°C and 200°C are shown in Fig. 6b and c. The surface consists of an assembly of perylene microcrystals which seem to be interconnected. The morphology may therefore be described as a crystal network. For a device cooled to -100°C we also observed crystal formation comparable to that in the device annealed at 95°C . In this case, it is unclear whether crystallisation occurred during cooling or reheating.

3.5. Morphology–performance relationship

The EQE of all treated devices was measured before and after treatment. The shape of the EQE spectra was practically unchanged after annealing, but the absolute value was always larger. The EQE shows a maximum increase of 49% for the device annealed at 95°C , which is shown in Fig. 8.

We have shown above that a network of the perylene crystals is formed as a result of thermal annealing. Horowitz et al. have produced evidence that similar perylene derivatives show n-type conduction [29]. Due to the higher degree of order the conductivity of the crystals of the perylene is likely to be higher than in perylene microdomains distributed within MEH-PPV, which has been successfully used as a hole transporter [14,15]. The formation of an electron conducting perylene crystal network should therefore enhance the electron transport and thereby increase the EQE.

4. Conclusions

We have shown that the EQE of MEH-PPV photovoltaic cells is increased by the introduction of a soluble perylene derivative into the polymer. Upon annealing such blend devices show a further enhancement of the EQE which has been attributed to the formation of an electron conducting network of interconnected perylene microcrystals.

These results have strong implications for the feasibility of device structures containing crystals or large rigid molecules such as nanotubes, which up to now have been considered inappropriate as photovoltaic materials, though desirable for their photophysical and transport properties.

Acknowledgements

Financial support from the Friedrich Naumann foundation and the European Commission TMR (SELOA-Network and Marie Curie Fellowship) and Brite-Euram OSCA program is gratefully acknowledged. R.L. is grateful for funding from the Fonds National de la Recherche Scientifique, Belgium. We would also like to thank Peter Ho and Devin MacKenzie for useful discussions.

References

- [1] J. Zhao, A. Wang, M.A. Green, *Appl. Phys. Lett.* 73 (1998) 1991.
- [2] J.H. Burroughes, D.D.C. Bradley, A.R. Brown, R.N. Marks, K. Mackay, R.H. Friend, P.L. Burns, A.B. Holmes, *Nature* 347 (1990) 539.
- [3] D. Braun, A.J. Heeger, *Appl. Phys. Lett.* 58 (1991) 1982.
- [4] N.C. Greenham, S.C. Moratti, D.D.C. Bradley, R.H. Friend, A.B. Holmes, *Nature* 365 (1993) 628.
- [5] Y. Yang, Q. Pei, A.J. Heeger, *J. Appl. Phys.* 79 (1996) 934.
- [6] N. Tessler, N.T. Harrison, R.H. Friend, *Adv. Mater.* 10 (1998) 64.
- [7] F. Garnier, R. Hajlaoui, A. Yassar, P. Srivastava, *Science* 265 (1994) 1684.
- [8] Y. Yang, A.J. Heeger, *Nature* 372 (1994) 344.
- [9] A.R. Brown, A. Pomp, C.M. Hart, D.M. Deleeuw, *Science* 270 (1995) 972.
- [10] A. Dodabalapur, Z. Bao, A. Makhija, J.G. Laquindanum, V.R. Raju, Y. Feng, H.E. Katz, J. Rogers, *Appl. Phys. Lett.* 73 (1998) 142.
- [11] H. Sirringhaus, N. Tessler, R.H. Friend, *Science* 280 (1998) 1741.

- [12] N. Tessler, G.J. Denton, R.H. Friend, *Nature* 382 (1996) 695.
- [13] F. Hide, B.J. Schwartz, M.A. DiazGarcia, A.J. Heeger, *Conjugated polymers as solid-state laser materials*, *Synth. Met.* 91 (1997) 35.
- [14] J.J.M. Halls, C.A. Walsh, N.C. Greenham, E.A. Marseglia, R.H. Friend, S.C. Moratti, A.B. Holmes, *Nature* 376 (1995) 498.
- [15] G. Yu, J. Gao, J.C. Hummelen, F. Wudl, A.J. Heeger, *Science* 270 (1995) 1789.
- [16] L.S. Roman, M.R. Andersson, T. Yohannes, O. Inganäs, *Adv. Mater.* 9 (1997) 1164.
- [17] L.S. Roman, L. Mammo, A.A. Pettersson, M.R. Andersson, O. Inganäs, *Adv. Mater.* 10 (1998) 774.
- [18] R.H. Friend, G.J. Denton, J.J.M. Halls, N.T. Harrison, A.B. Holmes, A. Köhler, A. Lux, S.C. Moratti, K. Pichler, N. Tessler, K. Towns, *Synth. Met.* 84 (1997) 463.
- [19] J.J.M. Halls, R.H. Friend, *Synth. Met.* 85 (1997) 1307.
- [20] H. Antoniadis, B.R. Hsieh, M.A. Abkowitz, S.A. Jenekhe, M. Stolka, *Synth. Met.* 62 (1994) 265.
- [21] W.R. Salaneck, *Philos. Trans. Roy. Soc. London Ser. A* 355 (1997) 789.
- [22] J.J.M. Halls, K. Pichler, R.H. Friend, S.C. Moratti, A.B. Holmes, *Appl. Phys. Lett.* 68 (1996) 3120.
- [23] N.S. Sariciftci, L. Smilowitz, A.J. Heeger, F. Wudl, *Science* 258 (1992) 1474.
- [24] M. Granström, K. Petritsch, A.C. Arias, A. Lux, M.R. Andersson, R.H. Friend, *Nature* 395 (1998) 257.
- [25] J.C. deMello, H.F. Wittmann, R.H. Friend, *Adv. Mater.* 9 (1997) 230.
- [26] J.J. Dittmer, *Determination of Absolute Photoluminescence Efficiency for Scattered Light*, unpublished results.
- [27] N. Chawdhury, A. Köhler, M.G. Harrison, D.H. Hwang, A.B. Holmes, R.H. Friend, *The Effects of H₂O and O₂ on the Photocurrent Spectra of MEH-PPV*, *Synthetic Metals* 102 (1999) 871.
- [28] J.J.M. Halls, *Photoconductive properties of conjugated polymers*, Cavendish Laboratory, Ph.D. Thesis, University of Cambridge, 1997.
- [29] G. Horowitz, F. Kouki, P. Spearman, D. Fichou, C. Nogue, X. Pan, F. Garnier, *Adv. Mater.* 8 (1996) 242.